

FRI-1.417-1-MEMBT-07

---

## OPTIMAL BUILD INCLINATION IN 3D PRINTING – SHELL ECO– MARATHON RAPID PROTOTYPING CAR PARTS CASE<sup>7</sup>

---

**Assist. Prof. Emil Yankov, PhD**

Department of Material Science and Technology  
University of Ruse, Bulgaria  
Phone: 082 888 205  
E-mail: eyankov@uni-ruse.bg

**Master Eng. Dimitar Kamarinchev, PhD student**

Department of Material Science and Technology  
University of Ruse, Bulgaria  
Tel.: 082-888-311  
E-mail: dkamarinchev@uni-ruse.bg

**Assoc. Prof. Roussi Minev, PhD**

Department of Material Science and Technology  
University of Ruse, Bulgaria  
Tel.: 082-888-310  
E-mail: rus@uni-ruse.bg

**Senior Lecturer Ekaterin Minev, MEng, PhD**

Department of Informatics and Information Technologies  
University of Ruse, Bulgaria  
Phone: 082 888 210  
E-mail: eminev@uni-ruse.bg

**Abstract:** *The article describes accuracy and quality investigation in the field of rapid prototyping (RP) and parts design for eco-friendly racing car. The manufactured components have been produced with the help of various process chains comprising of: digital scanning, 3D CAD modeling, 3D printing with high-precision photo polymers by SLA technology, and selection of techniques for precision and conventional investment casting.*

*The optimisation of the accuracy and the quality improvement of the prototypes are the main technological problems revealed in the study. Particular attention has been paid to the influence of one of the basic technological parameters - the angle of inclination of the part within the build chamber of the SLA apparatus.*

**Keywords:** *Rapid prototyping, 3D printing, Eco-friendly car, SLA, Rapid investment casting*

### INTRODUCTION

The wide application of 3D printers in the fields of mechanical engineering, jewelry and medicine [1-6, 21-27] in recent years has caused a lot of research work about the possibility for obtaining accurate precision products. The factors that affect the accuracy of printing include the ongoing thermodynamic processes, which depend on the heating and cooling rates with subsequent internal stresses in the materials that can lead to defects. The present study describes an approach for determination of deformations caused by local heating and cooling during SLA 3D printing.

The paper describes the influence of the model placement in the workspace for reducing the micro-deformations. For this purpose, different assessment methods are used for system reliability

---

<sup>7</sup> Докладът е представен в секция Механика и машиностроителни технологии на 25 октомври 2019 с оригинално заглавие на български език: ОПРЕДЕЛЯНЕ НА ОПТИМАЛНИЯ ЪГЪЛ НА НАКЛОНА ЗА 3D ПЕЧАТ - СЛУЧАЙ НА БЪРЗО ПРОТОТИПИРАНЕ НА КОМПОНЕНТИ ЗА АВТОМОБИЛ „ШЕЛ ЕКО-МАРАТОН“

and efficiency [7, 8]. Another method is the application of optimisation mathematical method for finding the optimal solution [9, 13,14, 15, 16, 17, 18, 19, 20 and 22] by monitoring the influence of the manageable factors.

### EXPERIMENTAL METHODOLOGY

For the purpose of this study, a digital model with dimensions 20×20 mm and thickness 3 mm was designed. The part consists 500×500×500 μm micro cubical holes in 1000 μm steps (Fig. 1a). The models were saved in \*.OBJ format suitable for the 3D printing.

To determin the optimal orientation for printing the test parst were tilted at 0°, 30°, 45°, 60°, 75° and 90° angles relative to the X-Y building table (Fig. 1b). The printing of the models was accomplished on a 3D printer Formlabs 2.0 (Fig. 3a).

The building material was the photopolymer Standart Black with precision of printing along the Z-axis 25 μm. The observation of the physical models was carried out with an optical microscope Carl Zeiss Jena at optical magnification ×6.3 (Fig. 2b). For the linear measurments, the microscope was equipped with 5MP digital camera and S-EYE software (Fig. 3a).

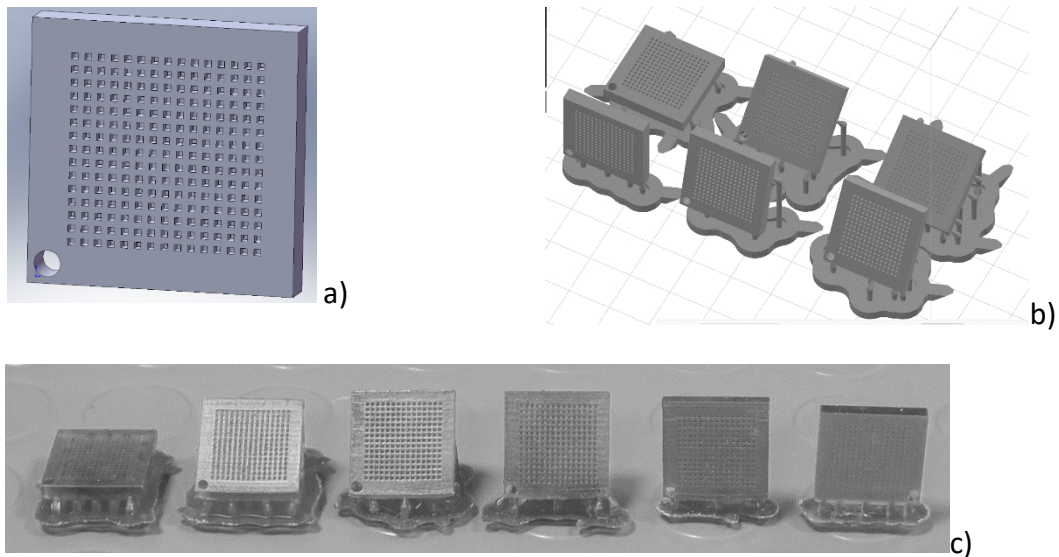


**Fig.1.** Prototype models: a) CAD model, b) orientations for printing; c) printed models.

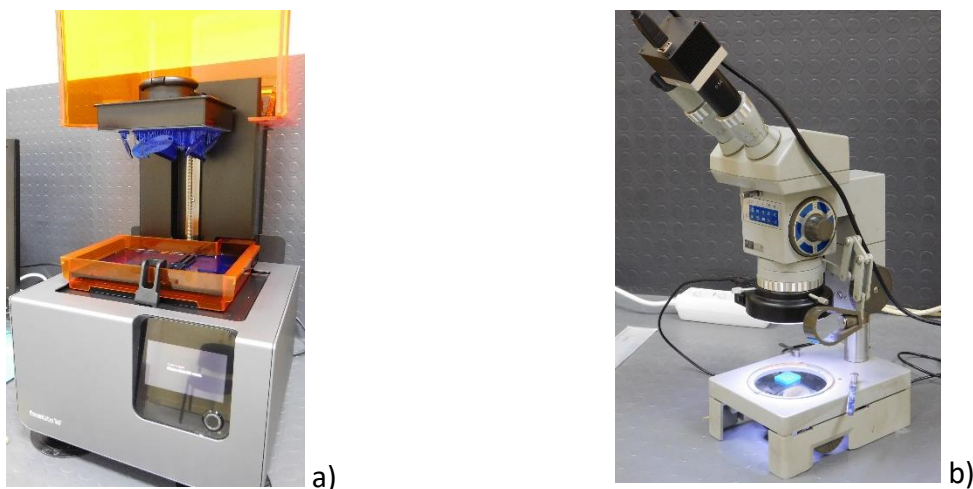


**Fig.2.** Used equipment: a) 3D printer Formlabs 2, b) microscope Carl Zeiss Jena.

The dimensions of the printed models were measured and compared with those of the digital models. For the evaluation of the deviations, the sizes and positions of the reference cubes were used

(Fig. 3b) [10, 11, 12]. Where  $X_i$  and  $Y_i$  are the coordinates of the center of each micro square on the digital model, while  $X_{i,j}$  and  $Y_{i,j}$  are the coordinates of the center of each micro square on printed model. The relative deformations  $\epsilon_X$  and  $\epsilon_Y$  were calculated by these dependencies:

$$\epsilon_X = \frac{\Delta X}{X_i} = \frac{X_{i,j} - X_i}{X_i}, \quad \epsilon_Y = \frac{\Delta Y}{Y_i} = \frac{Y_{i,j} - Y_i}{Y_i},$$

Micro displacements were measured and relative deformations were calculated in directions X and Y. On that basis, colored cards of the deviations were built showing relative deviations on each cell against the reference digital model.

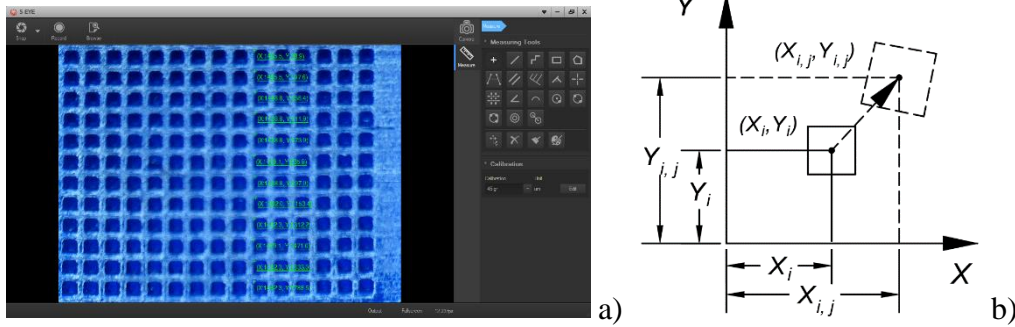


Fig.3. Determination of size deviations: a) measuring the part, b) determination of deformations.

### EXPERIMENTAL RESULTS

The data was processed and colour cards of deviations were created. (Fig. 4, Fig. 5).

When printing at  $0^\circ$  (horizontally) the deviations in X direction change sharply from extension to compression from first to second column (Fig. 4a).

For all other angles, the maximum compression is at the first column (Fig. 4 b, c, d, e and f). This area is the closest one to the supporting pillars, which influence could be the reason for the deviations from the nominal sizes. As the layers grow, the deviations in all inclined models change gradually through zero to the maximum particular extension.

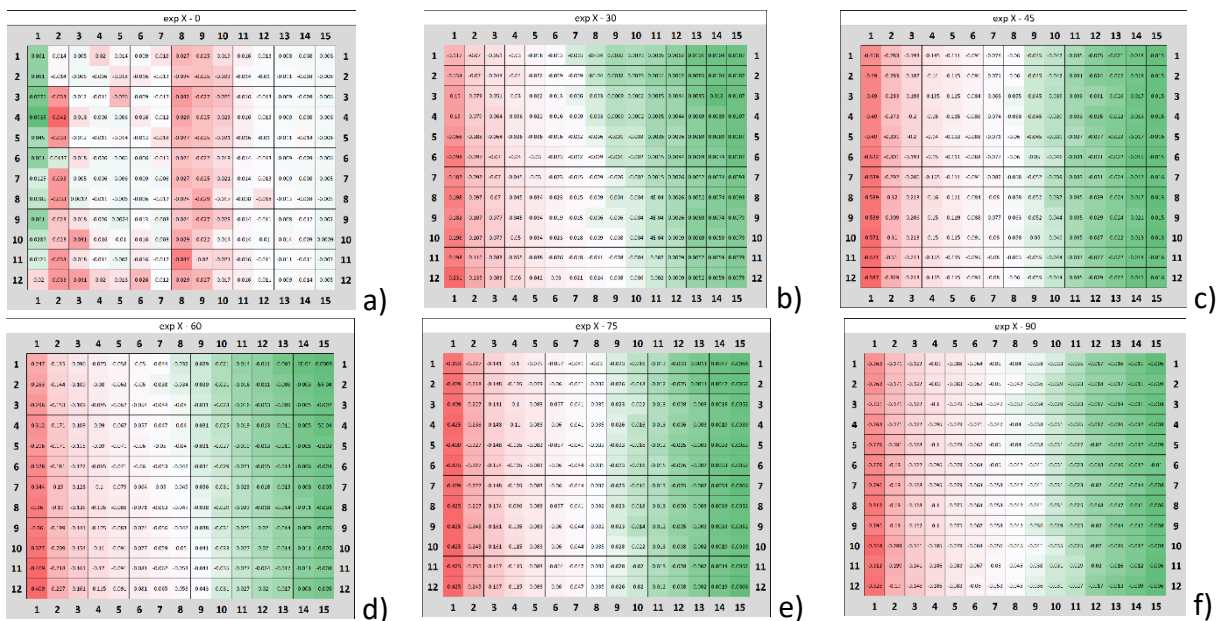


Fig. 4 Colour cards of the deviations in direction X: a)  $0^\circ$ , b)  $30^\circ$ , c)  $45^\circ$ , d)  $60^\circ$ , e)  $75^\circ$ , f)  $90^\circ$ .

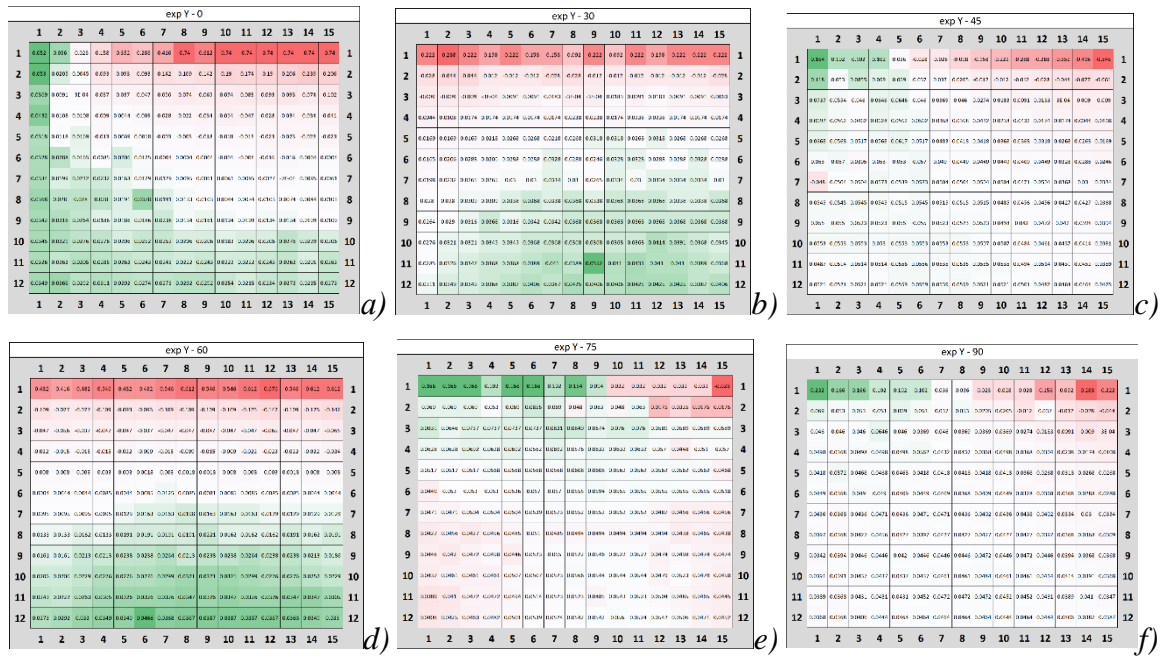


Fig. 5 Colour cards of the deviations in direction Y: a) 0°, b) 30°, c) 45°, d) 60°, e) 75°, f) 90°.

In the Y direction, compressions was also observed in the first row of all the printed models (Fig. 5). With the increasing of the height of the construction the deviations became positive, i.e. extension. The compression in the first row could be again the nearby supporting pillars. As the 3D printing layers increase, deviations also increase. This phenomenon is established also in the X direction, which is due to systematic error. This error is commensurate with the accuracy of the printer and with each following layer is accumulating, affecting the increase in the size of the squares. To determine the boundaries of deviations in X and Y directions, graphical dependencies were built for all inclinations of printing (Fig. 6, Fig. 7). In red is the maximum deviation value, and with purple is the minimum deviation value. At 0° printing, the deviations in X direction have the smallest range from -0.042 to 0.0935 (Fig. 6a). The reason is the small number of layers in height hence the small amount of the accumulated systematic error. When printing with 30° to 45° the deviations acquire maximum range of -0.588 to -0.012. The increasing of the printing angle to 90° results in a smooth decreasing of the deviations in the range of -0.344 -0.006174, which values are higher than those at 0° and 30°. In direction Y, the deviations of the sizes are of greater value (Fig. 7) than those in direction X except at 75° (Fig. 7e). The higher deviations in Y are at printing angles 0°, 45° and 60°. At 0° they are the highest and in range of -0.74 to 0.054. The lower deviations of the sample are obtained at printing of 30°. At printing angle of 75°, they are the smallest in the interval from -0.02 to 0.16. The reason for the higher deformation in direction Y is not only the systematic error in the Y axis, but also the layer-by-layer building up of the model along the Z axis.

Moving in Z axis leads to accumulation of errors in printed model. Furthermore, when building the model layer by layer each time the photopolymerised layer detaches from the silicone of the bath causes micro-tensile stresses on the already built model. This micro-tensile stresses cause an increase in the size in direction Y and a decrease in direction X. That explains the mostly negative deformation values in direction X and the positive ones in direction Y.

In order to find the best option for the angle of printing a comparative analysis was carried out for the positive and negative deformation deviations in directions X and Y (Fig. 8). For the purpose of the presented study the minimum and the maximum values of the deformation deviations are taken - $\epsilon_X(-)$ ,  $\epsilon_Y(-)$ ,  $\epsilon_X(+)$ ,  $\epsilon_Y(+)$  in X and Y. From the comparative analysis of the minimum and maximum deformation deviations in direction X is established that the smallest range of deviations in sizes is obtained at printing angle of 0°, while the largest range of deviations is at printing angle of 45° of the sample model. In Y direction the minimum and maximum deformation deviations are at 75° and 0° correspondingly.

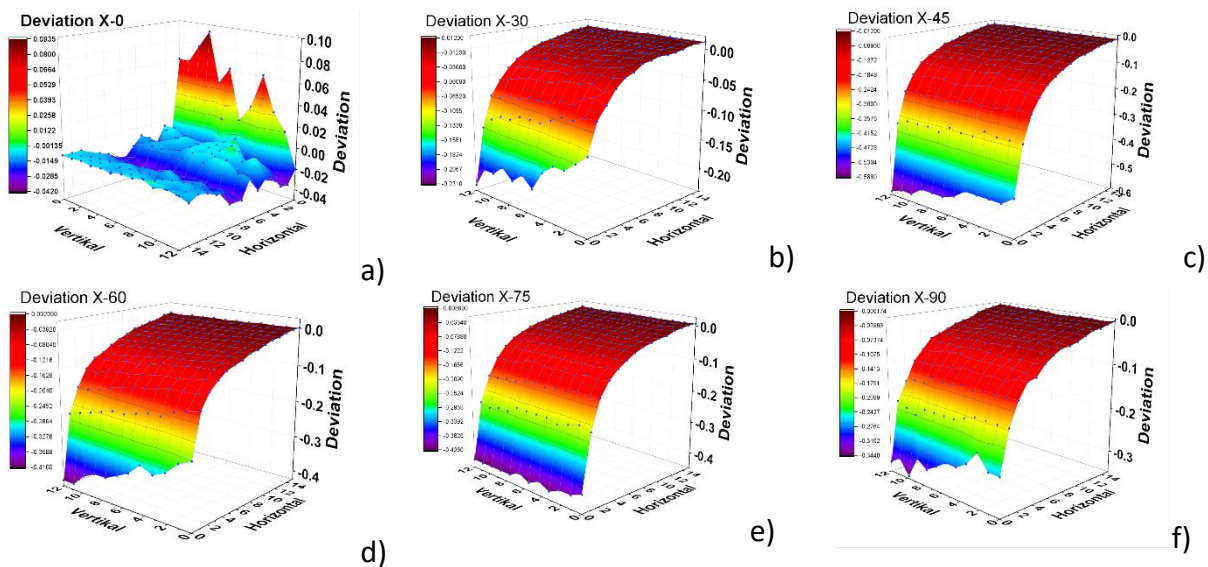


Fig. 6. Deviation of deformations in direction X: a) 0°, b) 30°, c) 45°, d) 60°, e) 75°, f) 90°.

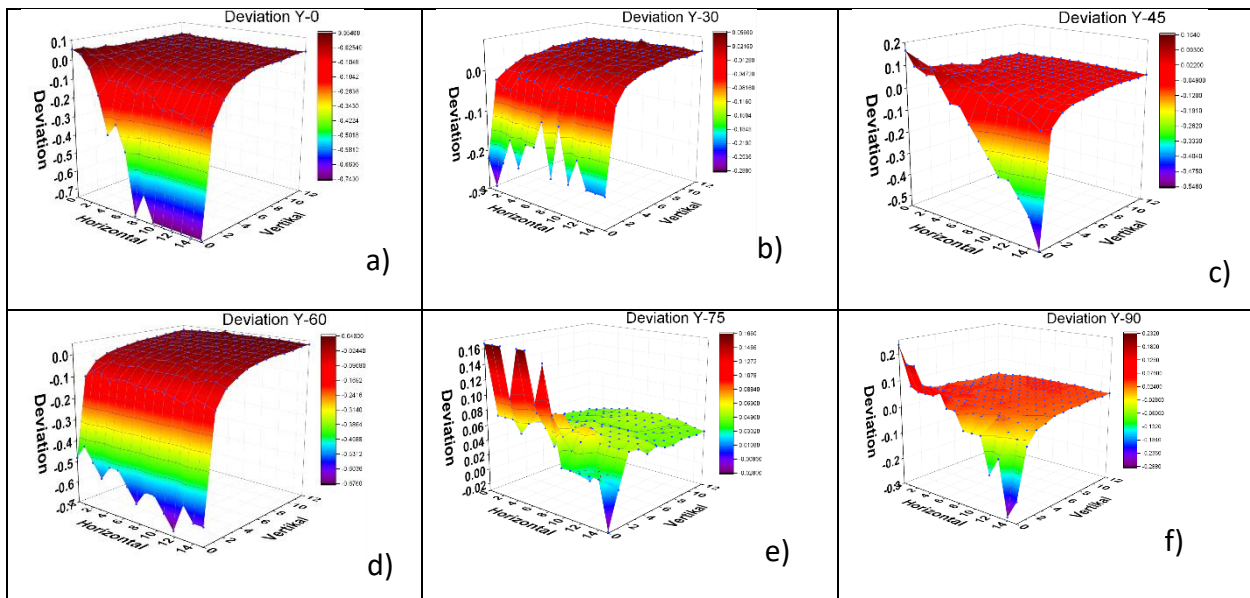
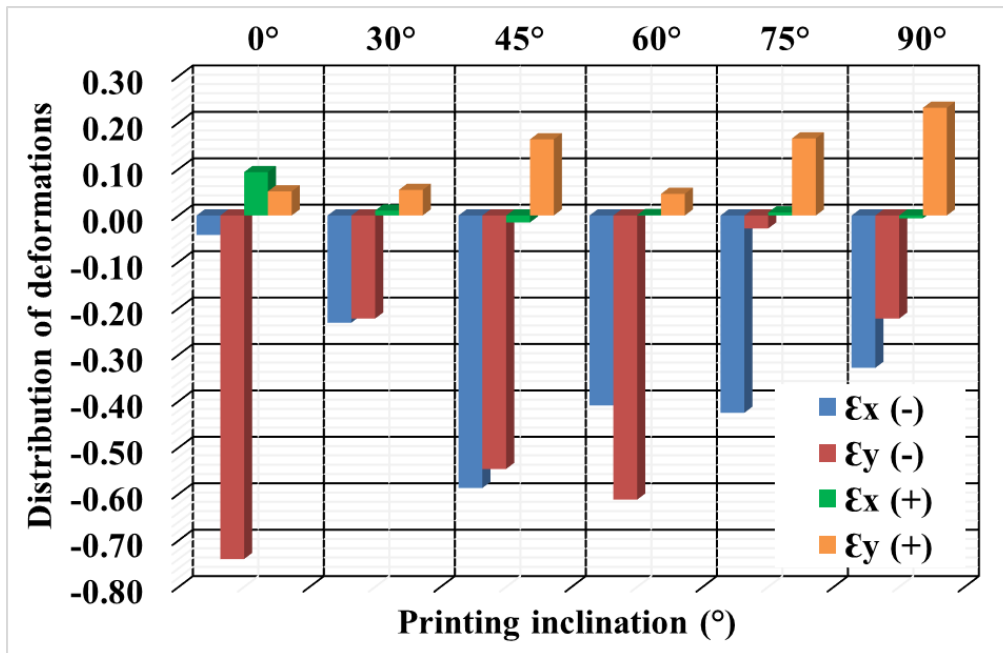


Fig. 7. Deviation of deformations in direction Y: a) 0°, b) 30°, c) 45°, d) 60°, e) 75°, f) 90°.

From the comparative analysis of the minimum and maximum deformation deviations in direction X is established that the smallest range of deviations in sizes is obtained at printing angle of 0°, while the largest range of deviations is at printing angle of 45° of the sample model. In Y direction the result shows minimum deviation at 75° and maximum at 0°.



*Fig. 8. Comparative diagram of deformation deviations along the upper and lower boundaries in directions X and Y.*

An analysis of the deformation deviations is conducted also between the negative values of both directions X and Y, as well as between the two positive ones. Their sum is also taken into account for the evaluation of the deviation. From the analysis of the negative deviations in directions X and Y is established, that the smallest range is obtained at printing angle of 30°, while the largest at 45°. For the positive deformation deviations in directions X and Y the lowest value is obtained at the printing angle of 60°, while the largest at the printing angle of 90°.

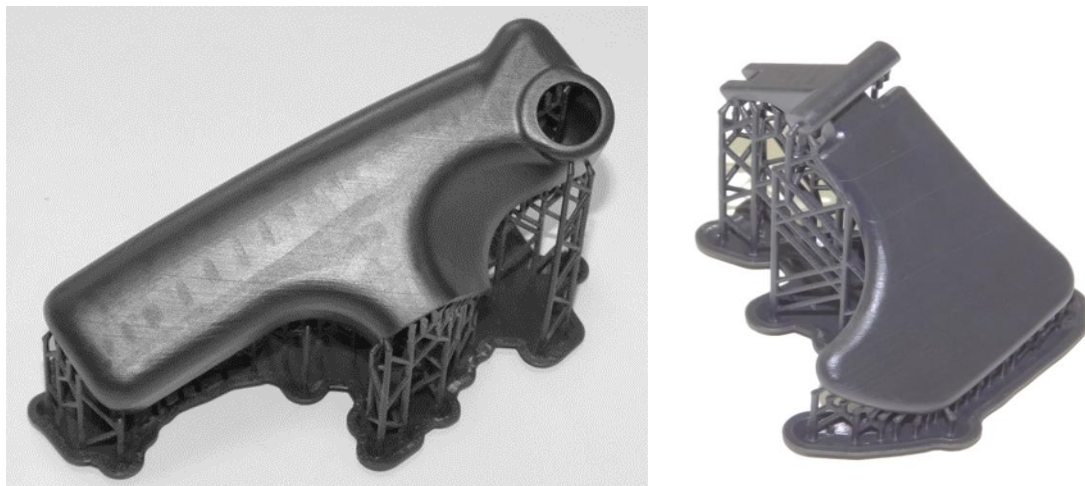


*Fig. 9. 3D models made by SLA metod of printing.*

To choose the optimal angle for printing the complex deformation behaviour in directions X and Y is taken into account. The outcome is that the smallest deformation deviation is at printing angle of 30°.

To confirm the experimental results shell models at printing angle 30° were produced (Fig. 9). The results shows that the building of shell models at proposed optimal angel is satisfactory.

## CONCLUSIONS

1. The optimal angle at which low deformation deviations in directions X and Y are observed is 30°, where these deviations are in the range of 0.243 and 0.344 respectively;
2. The minimum deformation deviations in direction X are established at an angle of printing of 0°, while those in direction Y at an angle of printing of 75°;
3. The maximum deformation deviations in direction X are established at an angle for 3D printing of 45°, while those in direction Y at an angle for 3D printing of 0°.
4. The deformation deviations in direction X are smaller than those in the direction Y except for an angle of printing at 75°. The reason is the matching of direction Y with the axis of motion Z, which axis is the factor for determining the thickness of the layer. In addition to that, at the axis Z is also carried out the peeling of the photopolymerized layer which causes micro-tensile stresses in the built model and leads to the increasing of the sizes in direction Y, as well as reducing of the sizes in direction X.

## ACKNOWLEDGMENTS

The presented research and the participation in this scientific conference were implemented with the financial support of the Research Fund at University of Ruse „Angel Kanchev“ by contract № 2019-MTФ-02 and project FNI 2019-RU-08 for Concept for Research Laboratory „LAYERED, ENERGY ASSISTED DIGITAL TECHNOLOGIES”.

## REFERENCES

- [1] William S. Land II, Z. Bin, Z. Ziegert and D. Angela, 43rd Proceedings of the North American Manufacturing Research, Institution of SME (Procedia Manufacturing), Volume 1, Pages 393–403 (2015).
- [2] I. Gajdoš et al., "Surface Finish Techniques for FDM Parts", Materials Science Forum, Vol. 818, pp. 45-48, (2015) DOI: 10.4028/www.scientific.net/MSF.818.45.
- [3] I. Gajdoš, I. Maňková, T. Jachowicz, A. Tor-Swiatek, Proceedings of 8th International Engineering Symposium at Bánki, (ISBN: 978-615-5460-95-1), Paper 32, (2016).
- [4] I. Gajdoš, E. Kaščák, E. Spišák and J. Slota, (Engineering Materials), Vol. 635, pp. 169-173, (2015), DOI: 10.4028/www.scientific.net/KEM.635.169..
- [5] H. Y. Yu, D. D. Ma, B. L. Wu, Nan Fang Yi Ke Da Xue Xue Bao (Journal of Southern Medical University), 37 (5) 668-672 (2017).
- [6] M. A. Kuss, R. Harms, S. Wu, Y. Wang, J. B. Untrauer, M. A. Carlson, B. Duan, RSC Advances 7, 29312-29320 (2017).
- [7] Popov, G., Braynov, N., Balevsky, A., Estimation of Hard Real-Time System Workability, (2018) International Conference on High Technology for Sustainable Development, HiTech 2018 - Proceedings, art. no. 8566346, <https://www.scopus.com/inward/record.uri?eid=2-s2.0>.
- [8] Popov, G., Nenova, M., Raynova, K., Investigation of Reliability of Diversity Systems Through Stress-Strength Model Analysis, (2018) 2018 7th Balkan Conference on Lighting, BalkanLight 2018 - Proceedings, art. no. 8546869.
- [9] Popov, G., Simulation of Markov Processes through Chains with Complex States, (2018) International Conference on High Technology for Sustainable Development, HiTech 2018 - Proceedings, art. no. 8566393.
- [10]. N. Feschiev, V. Gagov, E. Minev, Conf. Proc. Avangard technologies and machine building materials, VMEI Gabrovo, 187-191 (1992).
- [11] B. Tomov, V. Gagov, N. Feschiev, E. Minev, Proc. of 9th Machine Tool Conference, University Politechnica of Bucharest, 9 264-269 (1994).

- [12] V. Gagov, Testing and Processing of Contemporary Materials, Ljubljana-Ruse-Gliwice, 125-136 (1997).
- [13] Upcraft S., Fletcher R. (2003) The Rapid Prototyping Technologies, Assembly and Automation, v.23 Iss: 4, DOI:10.1108/01445150310698634, pp.318-330.
- [14] Minev R., Minev E., Technology for Rapid Prototyping - Basic Concepts, Quality Issues and Modern Trends, Scripta Scientifica Medicinæ Dentalis, v2, Nol (2016) pp. 12-22.
- [15] E.Minev et al., The RepRap Printers for Metal Casting Pattern Making - Capabilities and Application. IN: On Innovative Trends in Engineering and Science (SFITES'2015), Kavala, Greece, Pamas Publishing House ISBN 978-954-8483-35-6 (2015) pp. 122-127.
- [16] Bredendick, F. (1969) Zur ermittlung von deformationen an verzerrten gittern. Wiss. Technical University Dresden vol 16, pp. 1473-1481.
- [17] Minev R.M., (2003) RP with Vacuum Investment Casting, 'Development in Rapid Casting.
- [18] Case Studies', Professional Engineering Publishing Ltd. (IMEchE), ISBN: 978-1-86058-390-2, pp. 92-104.
- [19] Minev E., Yankov E., Minev R. (2015) The RepRap Printer for Metal Casting Pattenmaking.
- [20] Capabilities and Application, VIII International conference "Advanced foundry technologies", Moskow (*Оригинално заглавие:* Труды VIII Международной научно-практической конференции „Прогрессивные легкие технологии“, НИТУ МИСиС, 16-20.11.2015 Москва), ISBN 978-5-9903239-3-3, pp.300-303.
- [21] Józwik, Jerzy & Tofil, Arkadiusz & Łukaszewicz, Andrzej. (2019). Application of modern measurement techniques for analysis of injection moulding shrinkage. 10.22616/ERDev2019.18.N294.
- [22] Yankov, Emil & Nikolova, Maria. (2019). Orientation of the Digital Model for SLA 3D Printing and Its Influence on the Accuracy of the Manufactured Physical Objects for Micro- and Nano Technologies. 10.1007/978-3-030-02257-0\_21.
- [23] Schaefer, Benjamin & Sonnweber-Ribic, Petra & Hassan, Hamad & Hartmaier, Alexander. (2019). Micromechanical Modeling of Fatigue Crack Nucleation around Non-Metallic Inclusions in Martensitic High-Strength Steels. Metals. 9. 1258. 10.3390/met9121258.
- [24] Charoula Kousiatza, Dimitris Tzetzis, Dimitris Karalekas, In-situ characterization of 3D printed continuous fiber reinforced composites: A methodological study using fiber Bragg grating sensors, Composites Science and Technology, Volume 174, 2019, Pages 134-141, ISSN 0266-3538, <https://doi.org/10.1016/j.compscitech.2019.02.008>.
- [25] Ryosuke Matsuzaki, Taishi Nakamura, Kentaro Sugiyama, Masahito Ueda, Akira Todoroki, Yoshiyasu Hirano, Yusuke Yamagata, Effects of Set Curvature and Fiber Bundle Size on the Printed Radius of Curvature by a Continuous Carbon Fiber Composite 3D Printer, Additive Manufacturing, Volume 24, 2018, Pages 93-102, ISSN 2214-8604, <https://doi.org/10.1016/j.addma.2018.09.019>.
- [26] Kam, Menderes & Saruhan, Hamit & İpekci, Ahmet. (2018). INVESTIGATION THE EFFECTS OF 3D PRINTER SYSTEM VIBRATIONS ON MECHANICAL PROPERTIES OF THE PRINTED PRODUCTS. 36. 655-666.
- [27] L. García-Guzmán, L. Távara, J. Reinoso, J. Justo, F. París, Fracture resistance of 3D printed adhesively bonded DCB composite specimens using structured interfaces: Experimental and theoretical study, Composite Structures, Volume 188, 2018, Pages 173-184, ISSN 0263-8223, <https://doi.org/10.1016/j.compstruct.2017.12.055>.